Atmos. Meas. Tech., 8, 33–42, 2015
www.atmos-meas-tech.net/8/33/2015/
doi:10.5194/amt-8-33-2015

Atmospheric Measurement Techniques
Open Access

Dual-channel photoacoustic hygrometer for airborne measurements: background, calibration, laboratory and in-flight intercomparison tests

D. Tátrai[1,2], Z. Bozóki[1,2], H. Smit[3], C. Rolf[4], N. Spelten[4], M. Krämer[4], A. Filges[5], C. Gerbig[5], G. Gulyás[6], and G. Szabó[1,2]

[1]University of Szeged, Department of Optics and Quantum Electronics, Szeged, Hungary
[2]SZTE-MTA Research Group on Photoacoustic Spectroscopy, Szeged, Hungary
[3]Forschungszentrum Jülich, Institute for Energy and Climate Research Troposphere (IEK-8), Jülich, Germany
[4]Forschungszentrum Jülich, Institute for Energy and Climate Research Stratosphere (IEK-7), Jülich, Germany
[5]Max Planck Institute for Biogeochemistry, Department of Biogeochemical Systems, Jena, Germany
[6]Hilase Ltd., Szeged, Hungary

Correspondence to: D. Tátrai (tatraid@titan.physx.u-szeged.hu)

Received: 12 April 2014 – Published in Atmos. Meas. Tech. Discuss.: 26 June 2014
Revised: 19 November 2014 – Accepted: 20 November 2014 – Published: 6 January 2015

Abstract. This paper describes a tunable diode laser-based dual-channel photoacoustic (PA) humidity measuring system primarily designed for aircraft-based environment research. It is calibrated for total pressure and water vapor (WV) volume mixing ratios (VMRs) possible during airborne applications. WV VMR is calculated by using pressure-dependent calibration curves and a cubic spline interpolation method. Coverage of the entire atmospheric humidity concentration range that might be encountered during airborne measurements is facilitated by applying an automated sensitivity mode switching algorithm. The calibrated PA system was validated through laboratory and airborne intercomparisons, which proved that the repeatability, the estimated accuracy and the response time of the system are 0.5 ppmV or 0.5 % of the actual reading (whichever value is the greater), 5 % of the actual reading within the VMR range of 1–12 000 ppmV and 2 s, respectively. The upper detection limit of the system is theoretically about 85 000 ppmV, limited only by condensation of water vapor on the walls of the 318 K heated PA cells and inlet lines, and was experimentally verified up to 20 000 ppmV. The unique advantage of the presented system is its applicability for simultaneous water vapor and total water volume mixing ratio measurements.

1 Introduction

Volume mixing ratios (VMRs) of both atmospheric water vapor (WV) and total water (TW) (i.e., WV plus cloud droplets and ice crystals) change dynamically in space and time while they influence various meteorological parameters and, as one of the most effective absorbers of infrared radiation, they have a great impact on the global climate (Solomon et al., 2007). Therefore, it is preferable to measure them continuously and simultaneously with high spatial and temporal resolution, and ideally with global coverage. A possible measurement method is to equip research or in-service aircraft with WV and TW VMR measuring instruments. The idea of implementing atmospheric humidity measuring instruments (possibly in combination with other research instruments) onboard in-service aircraft is gaining increasing attention, as they can potentially form a global atmospheric monitoring network. In Europe, the MOZAIC (Measurement of OZone and water vapour by AIrbus in-service airCraft; Marenco et al., 1998) project launched 20 years ago was the first step in this direction. The currently ongoing IAGOS (In-service Aircraft for a Global Observing System; IAGOS, 2014) project equips a growing number of in-service aircraft with instruments measuring atmospheric composition, including WV VMR. Upgrading these instruments to measure TW VMR as well is expected to be a major step in atmospheric research.

Within the CARIBIC (Civil Aircraft for the Regular Investigation of the atmosphere Based on an Instrumented Container; Brenninkmeijer et al., 2007) project, which is now a part of the IAGOS project, a container is in operation with a large number of measuring instruments, and one of them is the instrument developed at the University of Szeged that measures WV and TW VMR simultaneously. That instrument is a predecessor of the system presented here.

Besides conventional requirements like accuracy, selectivity and reliability, an aircraft-operated atmospheric humidity measuring instrument has to fulfill various special requirements as follows:

- Compliance with rigorous safety regulations any aircraft equipment has to meet.
- Fast response time because of the high cruising speed of the aircraft.
- High resistance against mechanical vibrations.
- Fully autonomous and reliable operation.
- Low weight in order to minimize the extra fuel consumption of the aircraft.
- Wide measurement range in order to cover WV- and TW-VMR values that can occur in the atmosphere during typical aircraft flights.

Probably, the last requirement in combination with a fast response time is the most demanding one, as humidity varies from 1–2 ppmV (in dry air at about 12 km in height; CARIBIC, 2014) to 50 000 ppmV (in most humid air at the ground level, typically under tropical conditions). Furthermore, in the low humidity range, the precision of the measurements should be in the sub-ppmV range with high accuracy in order to be able to provide high-quality data.

At the University of Szeged during the last several years, efforts have been made to develop a room temperature diode laser-based photoacoustic (PA) system called WaSul-Hygro into a form optimized for simultaneous WV and TW VMR measurements (Szakáll et al., 2006, 2007; Tátrai et al., 2013). In this paper, the latest version of this system is presented together with its laboratory calibration, a blind laboratory test at Research Center Juelich (FZJ), and blind in-flight comparisons during a measurement campaign where WaSul-Hygro was operated simultaneously with a wavelength-scanned cavity ring-down spectrometer (WS-CRDS; Chen et al., 2010) and a Lyman-α photofragment fluorescence (LPF) based hygrometer (Chen et al., 2010).

2 Experimental

2.1 The photoacoustic system

The PA effect is the conversion of electromagnetic radiation into acoustic waves (Bell, 1880, 1881). Whenever a gas absorbs intensity- or wavelength-modulated light, the absorbed light energy is converted into acoustic waves via non-radiative relaxation processes. These acoustic waves can be considerably amplified by using a properly designed PA cell, through which the analyzed gas sample flows, and by setting the light source modulation frequency to coincide with a selected acoustic resonance frequency of the PA cell. The generated and amplified acoustic wave can be detected by a sensitive microphone. The amplitude of the acoustic signal at the frequency of the modulation of the light source is proportional to the concentration of the light-absorbing molecules (McDonald et al., 1978). This amplitude is usually determined by using the lock-in signal processing technique. In the following, the determined lock-in value is referred to as the PA signal. In the case of weak absorption (when the Lambert–Beer law can be approximated by the linear term of its Taylor series), the PA signal is a linear function of the absorption coefficient, but when the relative absorbed light power in the PA cell (described below) is above approximately 10 %, the sensitivity starts decreasing, which can be observed as nonlinearity during calibration. The PA measurement technique has been discussed in detail in several publications (Castleden et al., 1981; Saarela et al., 2009; Schilt and Thevenaz, 2006; Bozóki et al., 2011).

The layout of WaSul-Hygro, which is placed in a 19 inch 3U height rack and which has a weight of about 15 kg, can be seen in Fig. 1. Its custom controlling electronics is based on a digital signal processor (DSP) and is programmed for signal generation, data acquisition and operational control. Its main parts are a diode laser current driver, a programmable gain dual-channel microphone amplifier, a synchronized sampling-based dual-channel digital lock-in detector, temperature stabilization units, both for the laser and the detection cells, and analog and digital inputs and outputs for sensor signal reading and controlling the supplementary components of the system.

The light source is a room temperature operated, optical fiber coupled, distributed feedback diode laser (NEL NLK1E5E1AA). To stabilize and set the emission wavelength, the laser temperature can be accurately adjusted and stabilized with the help of a Peltier cell and a thermistor, both built into the housing of the laser (Seufert et al., 2004), and by applying a PID (proportional-integral-derivative) control algorithm. The tuning range of the laser extends from 1391 to 1394 nm, where water vapor has several absorption lines, and the measurements were performed on the strongest one, i.e., at 1392.535 nm, where the maximum optical absorption coefficient of 1 ppmV VMR of water vapor is $3.7 \times 10^{-5}\,\mathrm{m}^{-1}$ at 1000 hPa pressure (Sharpe et al., 2004). The laser in the system is wavelength modulated: periodically on and off tuned to the peak of the absorption line. Such modulation is optimal for the detection of molecules having narrow absorption lines, while it reduces the level of PA signals generated by interfering broad absorption features of, e.g., large

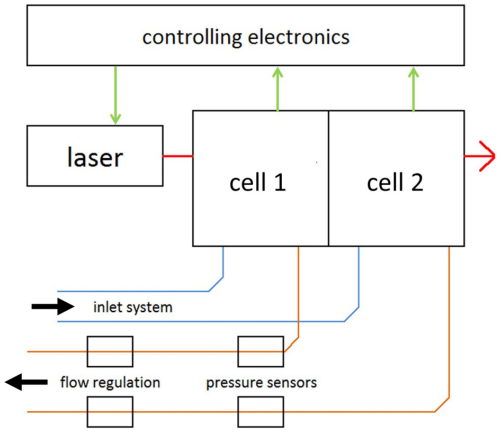

Figure 1. Schematic layout of the photoacoustic system. Green, red and black arrows indicate the electronic communication, laser beam propagation and gas flow directions, respectively. Blue and orange lines represent heated gas input and unheated gas output tubes, respectively.

molecules, atmospheric aerosols or pollutants condensing on the windows of the PA cell.

In order to maximize the sensitivity of the PA system, which is defined as the PA signal change caused by unit change in humidity, the amplitude of the laser modulation has to be optimized for the width of the absorption line (Szakáll et al., 2006), which strongly depends on the total gas pressure (Buldyreva et al., 2011). Taking into account that humidity typically decreases with decreasing air pressure (i.e., with increasing altitude), it is reasonable to optimize the laser modulation at a low pressure (in the current case, at 200 hPa) in order to have maximum sensitivity at low concentrations. Furthermore, the sensitivity of WaSul-Hygro decreases with decreasing pressure due to the acoustic properties of the PA cell. These two effects make the pressure dependence of the sensitivity rather complicated (Sect. 3.1.).

As result of the optimization, the laser is driven by a current waveform: $I(t) = I_0 + A \cdot \sin(2\pi \cdot f \cdot t)$, where $I_0 =$ 110 mA and $A = 5$ mA. The current tuning coefficient of the laser is 5 pm mA^{-1}; therefore, the offline wavelength is 1392.485 nm, which is at the very side of the absorption line at 200 hPa pressure. For best sensitivity, the modulation frequency has to be the same as the resonance frequency of the applied PA cell (more detail in Sect. 2.2.2). WaSul-Hygro includes two PA cells having the so-called longitudinal differential cell construction (Miklós et al., 2001) milled into a stainless steel block with the dimensions 10 cm × 10 cm × 4 cm (length by width by height). The cells are fixed together in a way that they have one common window through which the output excitation laser light from the first cell enters directly into the second cell. The cells are thermally isolated from their surroundings and equipped with a resistive heater and a PT100 resistance temperature detector. As sound velocity and, consequently, the acoustic resonance frequency of the PA cell are proportional to the square root of the temperature, in order to avoid uncontrolled variation of the acoustic resonance frequencies, the temperature of the cells is stabilized to 318 ± 0.1 K using a pulse-with-modulation algorithm. At this temperature, each cell has an acoustic resonance frequency of 4500 Hz.

The microphone signals are amplified electrically by an INA163 instrumentation amplifier; the gain of the amplifier can be programmatically set to either 60 or 600. The amplified microphone signals from both measuring cells are simultaneously and continuously sampled by the analog-to-digital converters (ADC) of the controlling electronics into sequences having a duration of about 2 s. This temporal resolution of the measurements was selected because 2 s is also the response time of the combination of the PA cells and the inlet system to sudden humidity variation.

As can be seen in Fig. 1, the gas handling of the PA system contains temperature-stabilized (heated to 318 ± 1 K) inlet lines, pressure sensors (Druck PMP 1400 series, 0–1500 hPa absolute) right after the PA cells, and mass flow controllers (Mykrolis Tylan FC2900, 0–1 sLpm (standard liter per minute)) that set the volume flow rates to 0.4 sLpm. During airborne operation, gas flow through the cells can be maintained either by the ram pressure at the sampling inlet of the aircraft or by a downstream vacuum pump. The former and latter cases are typically realized by a forward and sideward (or backward) facing sampling inlet, which can be used for TW and WV sampling, respectively. Elements of the gas handling are connected by 6 mm outer diameter stainless steel tubes and Swagelok connectors.

The measured PA signals, the pressures within the PA cells, and supplementary measurement information (like temperature values and self-checking results) are transferred to a data-logging PC connected to the electronics via a serial port. Software written in the LabVIEW graphical programming language (National Instruments) running on a PC calculates humidity values in real time from the measured data by using the calibration parameters (Sects. 2.2.4., 2.3., and 3.1.).

2.2 Special features of the photoacoustic system

Compared to its earlier versions, the presented system has several novel features, which were developed in order to improve the reliability of its operation.

2.2.1 Dual-channel operation

The dual-channel construction of the system can be used either to increase the signal-to-noise ratio of a single stream measurement by averaging the VMR readings of the two channels, or to measure humidity simultaneously in two different gas streams. In the latter case, the system can be used for simultaneous VW and TW (after evaporation in the tubes) VMR measurement whenever a proper inlet system is used,

like in the CARIBIC project (Brenninkmeijer et al., 2007), or for the validation and comparison of different sampling systems. As most of the setup (controlling electronics, laser) is common to the two cells, small differences between the VMR values in the sampling lines are expected to be more accurately measurable with the presented system rather than by using separate systems for each sampling line, since occasional laser control malfunctions or systematic errors would affect the two channels identically.

2.2.2 Sensitivity mode switching

Proportionality between the PA signal and the measured water vapor concentration holds over at least 5 orders of magnitudes, but the measurement range of the controlling electronics in its actual configuration cannot cover the entire range of interest, because the amplified microphone signal at high concentrations overloads the input of the ADC. To increase the measurement range of the electronics, a sensitivity mode (SM) switching algorithm is implemented in the DSP software, which automatically switches the microphone gain from 600 to 60 (or vice versa from 60 to 600) whenever the PA signal becomes higher (or lower) than a certain limit. Hysteresis between the switching limits is introduced in order to avoid frequent switching generated by small-scale signal fluctuations. The change in the SM makes it possible to extend the upper limit of the measurement range to 30 000 ppmV. Above this concentration, the AD converter saturates again; therefore, the PA signal has to be decreased further. This can be achieved by detuning the laser modulation frequency from the resonance frequency of the cell. This extends the measurement range by at least 1 order of magnitude, but above about, 85 000 ppmV water vapor starts condensing in the PA cell or in the sampling line, although due to occasional colder points can reduce this upper limit. However, such high WV VMR is really unlikely to occur during airborne measurements. Actually, the highest humidity level measured during the tests described in Sects. 2.4 and 2.5 was below 30 000 ppmV, so the off-resonant modulation was not applied.

At SM1 and SM2, the laser is modulated at the resonance frequency of the PA cell to achieve optimal performance, while at SM3, the modulation frequency is increased to 7950 Hz, where the sensitivity of the cell decreases by 1 order of magnitude.

To provide the functions listed above, the SM points are defined as follows: the sensitivity is lowered whenever the PA signal is greater than 66 % of the saturation value of the AD converter, and still can be lowered while increased whenever the PA signal is lower than 10 % of the saturation value of the AD converter, and still can be increased. An example can be found later on in Fig. 3.

2.2.3 Laser wavelength stabilization

The lower the pressure is, the narrower the water vapor absorption lines are, and consequently the wavelength stability of the laser becomes an increasingly critical issue. The wavelength of a properly temperature-stabilized laser can vary spontaneously due to the so-called ageing effects (Woodward et al., 1993); therefore, a wavelength locking method (WLM; Tátrai et al., 2013; Bozóki et al., 2013) with which the laser wavelength can be measured and set with at least 25 fm accuracy with 1 s execution time is applied. This wavelength uncertainty can cause less than 0.1 % error in the measured VMR values at any pressure. As the laser ageing effect becomes significant only on a rather long timescale, it is sufficient to perform the WLM only once during each flight, preferably after the Wasul-Hygro system is switched on and the aircraft is before take-off.

2.2.4 Real-time VMR calculation

The input parameters for the VMR calculation for both cells are the PA signals, the pressures in the cells, the actual SMs, and the calibration curves (Sects. 2.3 and 3.1), which form the calibration surface in the PA signal-pressure–VMR space. To calculate VMR, a two-step approach is used: first, VMRs are calculated from the PA signals for all 10 calibration pressures, and then, from the resulting data set, the actual VMR is determined by interpolation to the actual pressure using a cubic spline algorithm. The execution time of this method is on the order of milliseconds by using a general purpose PC or notebook giving the possibility of real-time VMR calculation.

2.3 Calibration of the PA system

In order to have a simple but reliable tool for the calibration through a wide concentration range and at various pressures, a setup shown in Fig. 2, including a home-made humidity generator (HG) and a reduced pressure stabilizer, was assembled around WaSul-Hygro. Its automatic operation is ensured by including a stepper motor-controlled needle valve, which together with the MFCs inside WaSul-Hygro and with a downstream pump reduces and stabilizes the pressure within the PA cells with ± 1 hPa accuracy. The pressure setting time is 2–4 s. The central part of the HG is a saturator with a spiral of 95 cm in length milled into a 12 cm $\times$ 12 cm $\times$ 6 cm copper block hermetically sealed from its surrounding. Thanks to an overpressure reduction tube, which is long enough to avoid back-diffusion of water vapor from ambient air and installed to eliminate the non-synchronizability of the MFC-s just before the saturator, the HG is operated close to atmospheric pressure.

At the beginning of the calibration, liquid nitrogen is poured into the HG, which cools down the saturator to around 120–140 K, and then the saturator slowly (during approxi-

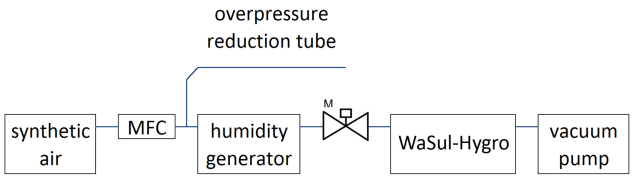

Figure 2. The schematic layout of the calibration system. MFC stands for mass flow controller and M is the stepper motor-controlled needle valve (see text for details).

mately 1.5 days) warms up to room temperature. Inside the saturator there is always ice or liquid water on the walls serving as a source of water vapor during warm-up, so the VMR will always correspond to the saturation pressure of water vapor at the temperature of the saturator. By measuring the temperature of the saturator with a PT100 resistance temperature detector and the gas pressure inside with a pressure sensor (Druck PMP 1400 series 0–1500 hPa absolute), the generated WV VMR can be calculated by using the Goff–Gratch equation (Goff and Gratch, 1946; WMO, 1983). This HG was calibrated against a chilled mirror hygrometer at the Hungarian National Office of Measures in the 1–25 000 ppmV range. During this calibration, an offset of 1.2 K was found between the measured temperature of the saturator and the actual dew/frost point. After correcting this offset, the repeatability of water vapor generation at any temperature was found to be ±0.5 % of the actual VMR or ±0.3 ppmV (the higher value applies).

The slow warm-up of the saturator makes it possible to vary the gas pressure repeatedly between 80, 130, 150, 200, 280, 370, 500, 650, 800 and 970 hPa, and also to repeat the PA measurements with the two different SMs. In this way, during a single warm-up of the HG, 20 different calibrations can be completed for each PA cell: each curve consists of five data points every 5 min.

2.4 Verification of the calibration

The PA system was blind tested at Research Center Jülich (Germany) at the Environmental Simulation Facility (ESF; Smit et al., 2000) chamber. The chamber has a test volume of about 500 L (80 cm × 80 cm × 80 cm), whereby relative humidity can be varied from about 95 down to 2 % over a temperature range between 300 and 200 K and a pressure range between 1000 and 100 hPa. Two reference instruments are connected to the chamber, an LPF hygrometer (Kley and Stone, 1978; Helten et al., 1998), which has an accuracy of ±3 % in the VMR range of 1–1000 ppmV, and a dew-/frost-point hygrometer (General Eastern, Type D1311R), which has a ±0.5 K uncertainty in the saturation temperature above 1000 ppmV.

During the measurements that were performed in the 2–12 000 ppmV VMR range at different pressures, the input lines for the two PA cells were joined by a tee connector. The air from the chamber was sampled through a 1.5 m length 1/8 inch heated stainless steel tube. Its inlet was placed as close as possible to the inlets of the reference instruments.

As the three instruments have different temporal resolutions, the results were interpolated to the time resolution of the PA system using the cubic spline method. From the resulting data sets, the relative deviation values, slopes of the cross plots, and the Pearson correlation values were determined.

2.5 Airborne tests

WaSul-Hygro was tested in a four-flight campaign dedicated to compare various systems measuring WV VMR within the DENCHAR (Development and Evaluation of Novel Compact Hygrometer for Airborne Research) project, which is part of the European Community's Seventh Framework Program EUFAR (European Facility for Airborne Research) funded project. The platform was a Learjet35A (Bombardier) research airplane operated by GFD GmbH (Hohn, Germany). Each flight was performed in the northern European airfield: above northern Germany, northern Poland, Denmark, southern Norway and the North Sea. Data were collected at different flight levels up to 13 km, so WaSul-Hygro was tested under tropospheric and lower stratospheric conditions as well. The PA system was compared to the FISH (Zöger et al., 1999) (Fast In-situ Stratospheric Hygrometer) instrument (measurement frequency of 1 Hz, a noise equivalent mixing ratio of 0.2–0.15 ppmV at 3 ppmV and a lower/upper detection limit of 0.18–0.13 / 1500 ppmV) during 3.6 h and with a commercially available PICARRO G2401-m WS-CRDS system (Picarro Inc., Santa Clara, CA, USA; Crosson, 2008). During the campaign, before and after each flight, FISH was calibrated against a chilled mirror hygrometer (MBW DP30) with the help of a saturation–dilution-based humidity generator. The WS-CRDS system simultaneously measures CO_2, CH_4, CO and H_2O, and it is specifically designed for flight operation; it was operated at 186.6 hPa (140 Torr). Its measurement time is about 2.5 s, and by lowering its sample flow rate down to 0.1 sLpm, it was able to measure at altitude level up to 12.5 km without using a sample pump upstream of the sample cell. The instrument itself is not a factory-calibrated one, but another WS-CRDS instrument was calibrated against a chilled mirror hygrometer (Dewmet, Michell instruments Ltd., UK) at the Max Planck Institute for Biogeochemistry, (Jena, Germany), and the calibration constants were transferred to all subsequently manufactured CRDS instruments by Picarro Inc. (Crosson, 2008). An accuracy better than 10 ppmV for mixing ratios less than 100 ppm and better than 200 ppmV above 10 000 ppmV was estimated from the chilled mirror hygrometer specifications (accuracy 0.2 °C dew point at 20 °C dew point, linearly increasing to 0.4 °C dew point at −60 °C dew point) assuming typical dew-point/pressure combinations. Precision was estimated to be 4 ppm or 1 % (whichever is larger). During the campaign,

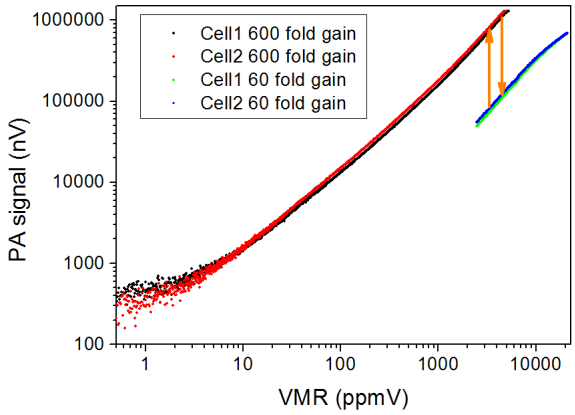

Figure 3. Calibration results at the pressure of 200 hPa. Arrows represent the SM switching points.

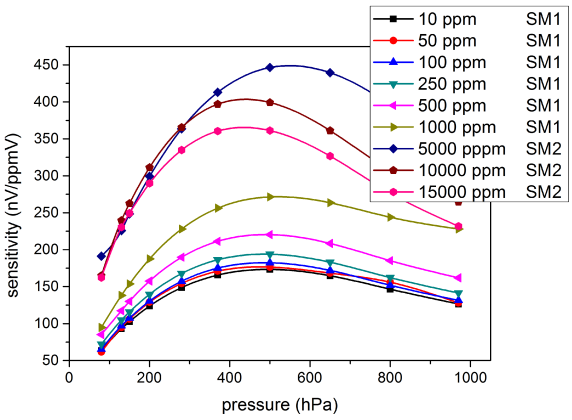

Figure 4. Dependence of the sensitivity of the PA system as the function of pressure at various VMRs. The sensitivities corresponding to 5000, 10 000 and 15 000 ppmV were measured at SM2 and up-scaled with a factor of 10 for better comparability, while the other curves were measured at SM1.

it was compared against the calibration standard used to calibrate FISH, revealing an offset of 14.5 ppmV that was subtracted from the CRDS flight data.

Unfortunately, for logistic reasons, the three instruments took their samples from three different inlets. During the campaign, the PA cells were configured to sample water vapor simultaneously from a single backward-facing aircraft inlet to measure WV VMR. The PA system was connected to the sampler by a heated stainless steel tube having an outer diameter of 1/8 inch and a length of 1.5 m. FISH was connected to a forward-facing inlet through a 0.5 m long, 10 mm inner diameter heated stainless steel tube to measure TW VMR, while the WS-CRDS system was connected to a forward-facing de-iced Rosemount total air temperature housing (model 102BX) through a FEP tube of 1 m in length and 1.58 mm inner diameter to measure WV VMR. For the Wasul-Hygro, the flow was provided by a downstream pump (MD1, Vacuubrand), while the WS-CRDS and FISH systems used the ram pressure provided by the samplers together with a downstream sampling pump.

For various reasons, large portions of the measured data are not suitable for intercomparison purposes, as follows. The central data-logging computer crashed repeatedly, causing data losses of 5 to 10 min periods. Considerable deviations between the readings of the three systems were observed during periods whenever the measured VMR varied rapidly, most probably due to the different response times of the sampling lines. WS-CRDS values below 50 ppmV had to be neglected, as their reliability is under discussion. The performance of FISH was acceptable only during the last two flights, due to a small internal leak that was discovered and fixed only after the second flight. During the campaign, FISH measured cloud-free data in the range 350 to 600 ppmV only for 4 min, and not at all above 600 ppmV. This amount of data above 350 ppmV is not enough for statistic conclusions, so these were neglected from the comparison. During the occasional presence of clouds, the FISH data had to be neglected, as their TW VMR data differed from the WV VMR reading of the other two instruments.

The comparable parts of the measured data were evaluated as done in the case of the ESF chamber comparison.

3 Results and discussion

3.1 Calibration

The calibration curves for the two WaSul-Hygro channels at one of the calibration pressures (200 hPa) together with the programmed SM switching points can be seen in Fig. 3. This curve was measured individually without periodically stepping the pressure for better visualization, but it overlaps the one used to program the calibration surface within the noise level. The measured sensitivities and noise levels (1σ) below 10 ppmV for the two measuring cells at 200 hPa pressure with 600-fold amplification of the microphone signal are 120 nV ppmV^{-1} and 54 nV and 118 nV ppmV^{-1} and 59 nV, respectively. At higher VMRs, similar sensitivities but higher noise levels (typically 0.5 % of the actual VMR reading) were found. Calibration curves at other pressures yield similar sensitivities and noise levels. From these results, it follows that the repeatability of the WV VMR measurements for either cell is 0.5 ppm or 0.5 % of the actual reading (whichever is greater). In Fig. 4, the sensitivity of the PA system as a function of pressure at different VMRs is shown. The dependencies are very similar for the two cells, but at higher VMRs, the sensitivity of the second PA cell is definitely lower due to the light attenuation in the first cell. Previously during the calibration procedure, only one calibration curve at a defined pressure was determined per PA cell, and the pressure-dependent sensitivity was determined at a certain VMR per PA cell (Szakáll et al., 2006). From Fig. 4, it can

Table 1. Results from comparisons of WaSul-Hygro with other instruments during laboratory and flight tests. In the case of the comparison with the WS-CRDS system above 4000 ppmV, there were no comparable numbers of data available, so the upper limits of the 2 and 5 % coincidences are certainly higher.

Reference instrument	Relative difference ranges from reference instruments (ppmV)			Pearson correlation coefficient	Slope of cross-plot line
	Within noise level	2 %	5 %		
ESF chamber	< 150	200–750	15–12 000	0.99948	1.015
WS-CRDS	< 300	1500–4000	100–4000	0.99986	1.047
FISH	< 20	NA	NA	0.9965	0.86

be clearly seen that the use of this simplifying assumption would lead to highly inaccurate VMR determination.

As calibration curves are not completely linear, partially due to the nonlinear behavior causing sensitivity decreases at higher concentrations, they have to be approximated with high (up to 10) order polynomials for both channels, for both SMs, at each pressure. These polynomials form the calibration surface, as mentioned before (Sect. 2.2.4.).

The VMR calculation method applied during laboratory tests showed traceability to the humidity generator within less than 0.5 % ± 0.5 ppmV at any VMR-s and at any pressures for both PA cells.

3.2 Laboratory intercomparison

During the laboratory measurements at the ESF chamber, the VMR values measured by the two channels of the PA system coincided within the noise level or within 0.5 %. These results are practically identical to the observed ones during laboratory calibration. One representative result of the laboratory intercomparison at FZJ is shown in Fig. 5a, where two SM switching points are also indicated. In Fig. 5b, the comparison cross plot between WaSul-Hygro and the reference instrument can be seen. The lower parts of Fig. 5a and b are the measured relative deviations as functions of time or VMR, respectively, with the horizontal line indicating ±5 % limits.

Values measured in the fast cooling and drying periods when the ESF chamber is far from its steady state and values in the case of fast VMR change when the chamber was not in its quasi steady state were omitted from the comparison. An example of these posterior omitted data in the range of 5–7000 ppmV can be seen in the deviation plot (Fig. 5b), where the loopy behavior indicates that the sampling line of the PA system could not follow the fast VMR variation in the chamber as fast as the reference instruments inside. It is important to note that the relative deviation in the presented case is still below 10 %. During the quasi steady-state parts of the measurements, the relative deviation (the difference between the VMR reading of WaSul-Hygro and the reference instrument divided by the WaSul-Hygro reading) is less than 5 %, or is

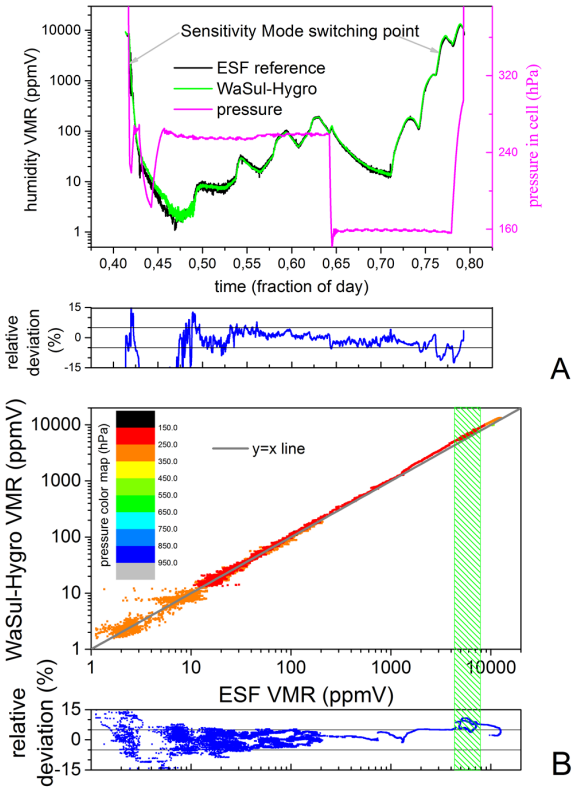

Figure 5. A representative measurement at the ESF chamber (5 May 2011). **(a)** is the time series of the measurements; **(b)** is the corresponding cross plot, where the pressure is coded by color and the green shaded area indicates the omitted loopy part.

noise level in the 15–12 000 ppmV range. Other parameters of comparison can be found in the first line of Table 1.

3.3 Airborne tests

During the flight tests, the noise level of the PA system and the deviation between the two sampling lines were almost the same as during laboratory intercomparison.

The comparisons of WaSul-Hygro with FISH and WS-CRDS instruments can be seen in Figs. 6 and 7, respectively,

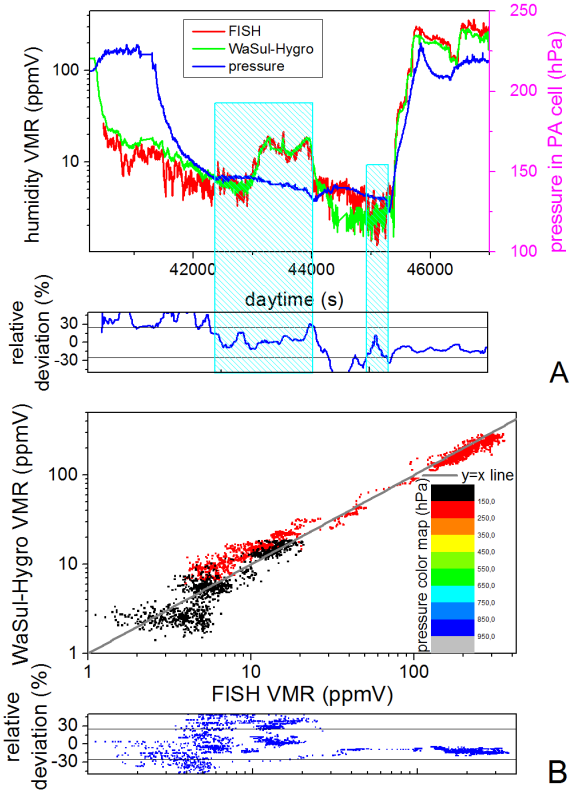

Figure 6. A representative comparison of WaSul-Hygro and FISH (DENCHAR flight, 31 May 2011). **(a)** is the time series of the measurements, where the blue shaded areas indicate when the two systems were measuring the same values within the noise level; **(b)** is the corresponding cross plot, where the pressure is coded by color.

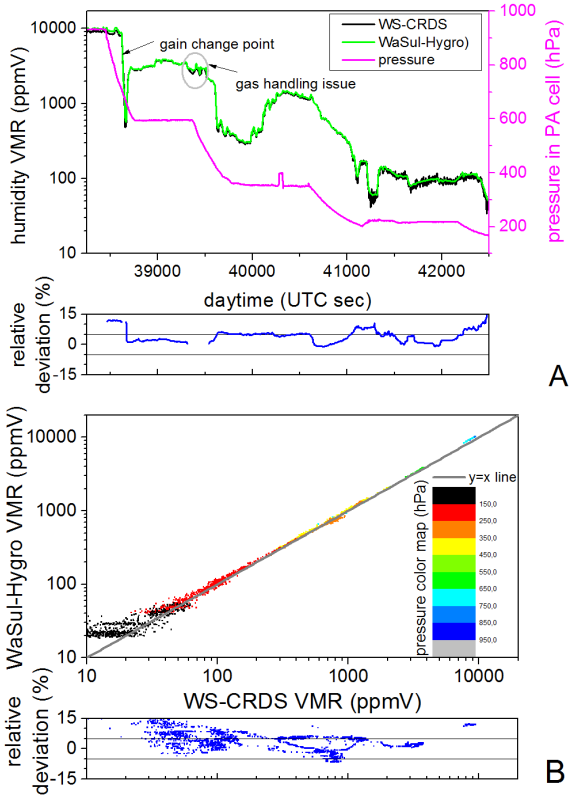

Figure 7. A representative comparison flight measurement of WaSul-Hygro and the WS-CRDS system (DENCHAR flight, 26 May 2011). **(a)** is the time series of the measurements; **(b)** is the corresponding cross plot, where the pressure is coded by color. The relative deviation below ∼ 30 ppmV is higher than 15 %, and is not indicated in plot **(b)**.

in a similar way as, previously, the results of the comparison at the ESF chamber, but in the case of the comparison with FISH, ±25 % limits are shown. An SM switching point and a period when the measurement results of the two instruments deviate considerably (most probably due to differences in the sampling lines) are marked in Fig. 7a. The comparison results can be found in detail in Table 1.

The slope of the cross plot between FISH and Wasul-Hygro deviates by about 20 % from the slope of the cross plot between Wasul-Hygro and the WS-CRDS system, which is close to the ideal of 1. The facts that the cross plot in Fig. 6b is close to linear and that the corresponding Pearson correlation coefficient is still high indicate that the deviation of FISH is most probably due not to a random effect or instrument malfunction such as noise. Furthermore, the deviation cannot be related to occasional occurrence of cloud droplets or ice crystals in the gas stream sampled by the TW inlet of FISH, because these events were carefully eliminated from the intercomparison. Therefore, it is rather a phenomenon that indicates that the WV VMR was indeed systematically different for the other sampling inlets, and definitely requires further studies.

3.4 Overall performance and outlook

Besides the performance parameters discussed above in detail, it is important to note that non-validated and therefore not presented tests show that the precision and accuracy values 18 months after the calibration did not vary significantly. These results still have to be verified and validated through more rigorous blind tests.

The actual size and weight of the system is acceptable on research aircraft, but in order to be mounted on an in-service one as a standard, these values still have to be improved. That is why a new controlling electronics is currently being developed, which, besides the significant size reduction, will be capable of real-time VMR calculation without the need for an external PC.

Acknowledgements. The authors would like to honor the memory of Cornelius Schiller (1961–2012), the former leader of the FISH development team and a worldwide recognized leading scientist of atmospheric humidity measurements.

The research leading to these results has received funding from EUFAR contract no. 227159. The project has been partially funded by TÁMOP-4.2.2.A-11/1/KONV-2012-0047 supported by the European Union and co-financed by the European Social Fund. The project has also been partially supported by the Hungarian Research and Technology Innovation Fund (OTKA), project no. NN109679. The research leading to these results has also received funding from the European Community's Seventh Framework Programme (FP7/2007-2013) under grant agreement no. 312311. D. Tátrai was partially supported by TÁMOP 4.2.4.A/2-11-1-2012-0001 supported by the European Union and Hungary and co-financed by the European Social Fund. For the operation of the Picarro WS-CRDS system, funding from IAGOS-ERI (In-service Aircraft for a Global Observing System – European Research Infrastructure, contract no. 212128), part of the EU's Seventh Framework Programme, was used.

Edited by: S. Malinowski

References

Bell, A. G.: On the production and reproduction of sound by light: the photophone, Am. J. Sci., 20, 305–324, 1880.

Bell, A. G.: Upon the production of sound by radiant energy, Philosophical Magazine and Journal of Science, 11, 510–528, 1881.

Bozóki, Z., Pogány, A., and Szabó, G.: Photoacoustic instruments for practical applications: present, potentials, and future challenges, Appl. Spectrosc. Rev., 46, 1–37, doi:10.1080/05704928.2010.520178, 2011.

Bozóki, Z., Tátrai, D., and Szabó, G.: Method and arrangement for wavelength monitoring of wavelength tunable light source and stabilizing based on absorption spectroscopic detecting; Hungarian patent, HU1100719 (A2), 2013.

Brenninkmeijer, C. A. M., Crutzen, P., Boumard, F., Dauer, T., Dix, B., Ebinghaus, R., Filippi, D., Fischer, H., Franke, H., Frieß, U., Heintzenberg, J., Helleis, F., Hermann, M., Kock, H. H., Koeppel, C., Lelieveld, J., Leuenberger, M., Martinsson, B. G., Miemczyk, S., Moret, H. P., Nguyen, H. N., Nyfeler, P., Oram, D., O'Sullivan, D., Penkett, S., Platt, U., Pupek, M., Ramonet, M., Randa, B., Reichelt, M., Rhee, T. S., Rohwer, J., Rosenfeld, K., Scharffe, D., Schlager, H., Schumann, U., Slemr, F., Sprung, D., Stock, P., Thaler, R., Valentino, F., van Velthoven, P., Waibel, A., Wandel, A., Waschitschek, K., Wiedensohler, A., Xueref-Remy, I., Zahn, A., Zech, U., and Ziereis, H.: Civil Aircraft for the regular investigation of the atmosphere based on an instrumented container: The new CARIBIC system, Atmos. Chem. Phys., 7, 4953–4976, doi:10.5194/acp-7-4953-2007, 2007.

Buldyreva, J., Lavrentieva, N., and Starikov, V.: Collisional Line Broadening And Shifting Of Atmospheric Gases; A Practical Guide for Line Shape Modelling by Current Semi-classical Approaches; Imperial College Press: London, UK, 2011.

CARIBIC: CARIBIC website, available at: http://www.caribic-atmospheric.com/, last access: 27 November 2014.

Castleden, S. L., Kirkbright, G. E., and Spillane, D. E. M.: Wavelength modulation in photoacoustic spectroscopy, Anal. Chem., 53, 2228–2231, doi:10.1021/ac00237a019, 1981.

Chen, H., Winderlich, J., Gerbig, C., Hoefer, A., Rella, C. W., Crosson, E. R., Van Pelt, A. D., Steinbach, J., Kolle, O., Beck, V., Daube, B. C., Gottlieb, E. W., Chow, V. Y., Santoni, G. W., and Wofsy, S. C.: High-accuracy continuous airborne measurements of greenhouse gases (CO_2 and CH_4) using the cavity ring-down spectroscopy (CRDS) technique, Atmos. Meas. Tech., 3, 375–386, doi:10.5194/amt-3-375-2010, 2010.

Crosson, E. R.: A cavity ring-down analyzer for measuring atmospheric levels of methane, carbon dioxide, and water vapor, Appl. Phys. B, 92, 403–408, doi:10.1007/s00340-008-3135-y, 2008.

Goff, J. A. and Gratch, S.: Low-pressure properties of water from −160 to 212 F, T. Am. Soc. Heat. Vent. Eng., 52, 95–122, 1946.

Helten, M., Smit, H. G. J., Straeter, W., Kley, D., Nedelec, P., Zöger, M., and Busen, R.: Calibration and performance of automatic compact instrumentation for the measurement of relative humidity from passenger aircraft, J. Geophys. Res., 103, 643–652, doi:10.1175/2007JTECHA975.1, 1998.

IAGOS: IAGOS website, available at: http://www.iagos.org, last access: 27 November 2014.

Kley, D. and Stone, E. J.: Measurement of water vapor in the stratosphere by photodissociation with Ly (a) (1216 A) light, Rev. Sci. Instrum., 49, 691–697, doi:10.1063/1.1135596, 1978.

Marenco, A., Thouret, V., Nédélec, P., Smit, H. G. J., Helten, M., Kley, D., Karcher, F., Simon, P., Law, K., Pyle, J., Poschmann, G., Wrede, R. V., Hume, C., and Cook, T.: Measurement of ozone and water vapor by Airbus in-service aircraft: The MOZAIC airborne program, an overview, J. Geophys. Res.-Atmos., 103, 25631–25642, doi:10.1029/98JD00977, 1998.

McDonald, F. A. and Wetsel Jr., G. C.: Generalized theory of the photoacoustic effect, J. Appl. Phys., 49, 2313–2322, doi:10.1063/1.325116, 1978.

Miklós, A., Hess, P., and Bozóki, Z.: Application of Acoustic Resonators in Photoacoustic Trace Gas Analysis and Metrology, Rev. Sci. Instrum., 72, 1937–1955, doi:10.1063/1.1353198, 2001.

Szakáll, M., Huszár, H., Bozóki, Z., and Szabó, G.: On the pressure dependent sensitivity of a photoacoustic water vapor detector using active laser modulation control, Infrared Phys. Techn., 48, 192–201, doi:10.1016/j.infrared.2006.01.002, 2006.

Szakáll, M., Csikós, J., Bozóki, Z., and Szabó, G.: On the temperature dependent characteristics of a photoacoustic water vapor detector for airborne application, Infrared Phys. Techn., 51, 113–121, doi:10.1016/j.infrared.2007.04.001, 2007.

Tátrai, D., Bozóki, Z., and Szabó, G.: Method for wavelength locking of tunable diode lasers based on photoacoustic spectroscopy, Opt. Eng., 52, 096104, doi:10.1117/1.OE.52.9.096104, 2013.

Saarela, J., Toivonen, J., Manninen, A., Sorvajärvi, T., and Hernberg, R.: Wavelength modulation waveforms in laser photoacoustic spectroscopy, Appl. Optics, 1, 743–748, doi:10.1364/AO.48.000743, 2009.

Schilt, S. and Thevenaz, L.: Wavelength modulation photoacoustic spectroscopy: Theoretical description and experimental results, Infrared Phys. Techn., 48, 154–162, doi:10.1016/j.infrared.2005.09.001, 2006.

Seufert, J., Fischer, M., Koeth, J., Werner, R., Kamp, M., and Forchel, A.: DFB laser diodes in the wavelength range from

760 nm to 2.5 µm, Spectrochim. Acta A, 60, 3243–3247, doi:10.1016/j.saa.2003.11.043, 2004.

Sharpe, S. W., Johnson, T. J., Sams, R. L., Chu, P. M., Rhoderick, G. C., and Johnson, P. A.: Gas-Phase Databases for Quantitative Infrared Spectroscopy, Appl. Spectrosc., 58, 1452–1461, doi:10.1366/0003702042641281, 2004.

Smit, H. G. J., Strater, W., Helten, M., and Kley, D.: Environmental simulation facility to calibrate airborne ozone and humidity sensors, Tech. Rep. Juel. Berichte No. 3796, Forschungszentrum Jülich, available at: http://www.fz-juelich.de/SharedDocs/Downloads/IEK/IEK-8/EN/ESF/ESF.pdf (last access: 27 November 2014), 2000.

Solomon, S., Qin, D., Manning, M., Chen, Z., Marquis, M., Averyt, K. B., Tignor, M., and Miller, H. L.: Climate Change 2007: The Physical Science Basis Contribution of Working Group I to the Fourth Assessment Report of the Intergovernmental Panel on Climate Change; Cambridge University Press, Cambridge, United Kingdom and New York, NY, USA, 2007.

WMO: WMO-Report No. 8, Measurement of atmospheric humidity, Guide to meteorological instruments and methods of observation, 5th Edn., World Meteorological Organization, Geneva, 5.1–5.19, 1983.

Woodward, S. L., Parayanthal, P., and Koren, U.: The effects of aging on the Bragg section of a DBR laser, Photonics Technology Letters, 5, 750–752, doi:10.1109/68.229794, 1993.

Zöger, M., Afchine, A., Eicke, N., Gerhards, M. T., Klein, E., McKenna, D. S., Mörschel, U., Schmidt, U., Tan, V., Tuitjer, F., Woyke, T., and Schiller, C.: Fast in situ stratospheric hygrometers: A new family of balloonborne and airborne Lyman-α photofragment fluorescence hygrometers, J. Geophys. Res., 104, 1807–1816, doi:10.1029/1998JD100025, 1999.